*Manuscript

The paper is submitted as an original article.

Title of the paper: "An open source lower limb model: hip joint validation"

Authors: L. Modenese, A. T. M. Phillips, A. M. J. Bull

Corresponding author: L. Modenese

Address: Imperial College London
Structural Biomechanics
Dept. Civil and Environmental Engineering,
Skempton Building,
South Kensington Campus,
SW7 2AZ London, UK

Email: l.modenese08@imperial.ac.uk

Telephone: +442075945963

Fax: +442075945934

Keywords: musculoskeletal model;
hip contact force;
leg model;
static optimization

Word count: 3578 words

Abstract

Musculoskeletal lower limb models have been shown to be able to predict hip contact forces (HCFs) that are comparable to *in vivo* measurements obtained from instrumented prostheses. However, the muscle recruitment predicted by these models does not necessarily compare well to measured electromyographic (EMG) signals.

In order to verify if it is possible to accurately estimate HCFs from muscle force patterns consistent with EMG measurements, a lower limb model based on a published anatomical dataset (Klein Horsman et al. 2007. Clin Biomech, 22. 239-247) has been implemented in the open source software OpenSim. A cycle-to-cycle hip joint validation was conducted against HCFs recorded during gait and stair climbing trials of four arthroplasty patients (Bergmann et al. 2001. J Biomech, 34, 859-871). Hip joint muscle tensions were estimated by minimizing a polynomial function of the muscle forces. The resulting muscle activation patterns obtained by assessing multiple powers of the objective function were compared against EMG profiles from the literature. Calculated HCFs denoted a tendency to monotonically increase their magnitude when raising the power of the objective function; the best estimation obtained from muscle forces consistent with experimental EMG profiles was found when a quadratic objective function was minimized (average overestimation at experimental peak frame: 10.1% for walking, 7.8% for stair climbing).

The lower limb model can produce appropriate balanced sets of muscle forces and joint contact forces that can be used in a range of applications requiring accurate quantification of both. The developed model is available at the website https://simtk.org/home/low_limb_london.

1. Introduction

Musculoskeletal models of the lower limb have been developed and used to investigate the biomechanics of the hip (Crowninshield et al., 1978), muscle architecture with respect to force generation (Arnold et al., 2010) and to aid in surgical considerations (Delp et al., 1990) including preclinical implant testing (Heller et al., 2001). The geometrical data used to implement these models have generally been inferred from anatomy books e.g. Seireg and Arvikar (1973) or cadaveric measurements e.g. Brand et al. (1982). Recently a new set of anatomical data was collected by Klein Horsman et al. (2007) on a single specimen. They applied the criterion of mechanical equivalence proposed by Van der Helm and Veenbaas (1991) to muscle discretization and reported muscle attachment positions. Joint kinematics and muscle contraction parameters were also measured, making this dataset particularly suitable for musculoskeletal model implementation. Models derived from this data have already been used and published (Klein Horsman, 2007; Cleather and Bull, 2010) although to the authors' knowledge only qualitative validation of the resulting models has so far been conducted (Koopman and Klein Horsman, 2008).

Two standard forms of validation are used in these models: the first is a direct measure of hip contact forces (HCFs), the internal forces transferred between the femoral head and the acetabulum of the pelvis, from instrumented implants taking measurements at the femoral head (Rydell, 1966; Davy et al., 1988; Bergmann et al., 2001) and the second is the use of electromyographic signals (EMG) as a surrogate for muscle force and activation patterns (Seireg and Arvikar, 1975; Pedersen et al., 1987; Glitsch and Baumann, 1997; Lenaerts et al., 2008).

Several investigators in the literature calculated HCFs (Paul, 1965; Seireg and Arvikar, 1975; Crowninshield et al., 1978; Hardt, 1978; Röhrle et al., 1984; Pedersen et al., 1987; Glitsch and Baumann, 1997; Lenaerts et al., 2008) but only a few of them (Brand et al., 1994; Lu et al., 1997; Heller et al., 2001; Stansfield et al., 2003) validated their model against experimental measurements obtained through instrumented prostheses. Considering just the studies based on hip joint instrumented prostheses, Brand et al. (1994) validated their model using a nonlinear optimization approach but the kinematic data used in their investigation was collected several weeks after the HCFs measurement. Heller et al. (2001) obtained good agreement between the calculated and the experimentally measured HCFs, but muscle forces were calculated using a linear criterion minimizing their sum; this criterion has been shown not to be suitable for accurate muscle activation pattern prediction in complex musculoskeletal models because it recruits fewer muscles than are documented in EMG studies (Yeo, 1976; Hardt, 1978; Pedersen et al., 1987), unless additional activation constraints are imposed (Crowninshield, 1978). Furthermore linear criteria seem to preclude antagonistic activity (Pedersen et al., 1987). Stansfield et al. (2003), used a double stage linear optimization technique (Bean and Chaffin, 1988) in order to enhance muscle synergism, but their model was unable to accurately reproduce the two-peaked nature of the HCFs during gait and the muscle activation patterns were not completely consistent with the EMG profiles. Considering the relative insensitivity of HCFs to differences in muscle load sharing (Brand et al., 1986; Stansfield et al., 2003), it may be possible to predict HCFs close to those measured *in vivo* based on sets of muscle forces and activation patterns inadequately supported by EMG measurements.

The aim of this investigation is to assess whether it is feasible using a musculoskeletal model to predict HCFs close to those measured *in vivo* (Bergmann et al., 2001) based on muscle forces whose activation patterns are supported by experimental EMG recordings. With this aim a lower limb model based on the anatomical dataset collected by Klein Horsman et al. (2007) is introduced and its performance assessed over a range of different muscle recruitment criteria through the following steps:

1. HCFs predicted by the model using the kinematic and kinetic data available in the literature (Bergmann et al. (2001), hereafter referred to as HIP98) are compared against *in vivo* measured HCFs (also from HIP98) for the two most frequent activities of daily living, level walking and stair climbing (Morlock et al., 2001).
2. Muscle forces and associated activation patterns estimated by the model producing the predicted HCFs are compared against experimental EMG measurements available in the literature for both activities.

Special attention is given to the influence of muscle synergism on both HCFs and muscle forces.

Methods

2.1 The musculoskeletal model

The lower limb musculoskeletal model used in this study was implemented using an anatomical dataset based on measurements on the right leg of a single cadaveric specimen (Klein Horsman et al., 2007). The model consists of 6 segments (pelvis, femur, patella, tibia, hindfoot and midfoot plus phalanxes) considered as rigid bodies onto which the muscles are attached (Fig. 1).

163 actuators are included in the model in order to represent 38 muscles, divided into 57 muscle parts composed of up to 6 bundles (Klein Horsman et al., 2007). The muscle paths are enhanced by via points and wrapping surfaces where the muscles are allowed to slide without friction. The muscle isometric strength F_{ISO} is considered to be proportional to the physiological cross sectional area and calculated using a maximum muscle tensile stress of 37 N/cm^2, chosen after Weijs and Hillen (1985) and Haxton (1944).

The unilateral model includes 5 joints. The hip is modeled as a ball and socket joint, the tibio-femoral joint is represented as a hinge and the ankle joint complex is composed of the talocrural and the subtalar joints, both revolute joints. The patella is dragged by the patellar ligament (assumed to be inextensible) along a circular path on a plane perpendicular to the patello-femoral axis; the patello-femoral axis is distinct from the flexion-extension knee axis. The positions of the joint centers, orientations of joint axes and description of patello-femoral mechanism are reported by Klein Horsman et al. (2007). The total degrees of freedom of the model are potentially twelve, but the subtalar joint was locked in the neutral position during the static optimization analysis reducing this number to eleven.

Some modifications were applied to the parameters reported by Klein Horsman et al. (2007). The insertion of *adductor magnus* (distal bundles) was moved from the tibia to the femur as there was no anatomical justification for the former attachment. The talocrural joint axis was moved with respect to the original position in order to allow the foot to align with the neutral position described by the International Society of Biomechanics when the rest position was assumed (Wu et al., 2002). Communication with one of the authors of the study (Klein

Horsman et al., 2007) has confirmed these alterations are required to provide functionality of the developed model.

2.2 Kinematics and Inverse dynamics

In order to obtain a cycle-to-cycle comparison of the HCFs calculated by the model with the experimental measurements, the kinematic and ground reaction forces reported in the HIP98 dataset were used to set up the numerical simulations. All of the normal speed walking and stair climbing trials available in HIP98 for each of the four different patients were investigated (see Table 1 for details). All these patients have previously been assessed by Heller et al. (2001) and subjects S1 and S2 by Stansfield et al. (2003).

A model representative of each subject was derived after mirroring the general right leg model, since the available kinematics describe the pelvis and left limb motion. The segment lengths were linearly scaled using scaling ratios calculated from the joint rotation centre and the bony landmark locations available in the HIP98 database, while the segment masses were manually set to the values published by Bergmann et al. (2001) after scaling the length of the segments. The generalized coordinates used to drive the subject specific versions of the model were obtained applying the algorithm described by Lu and O'Connor (1999) to the available marker data.

Using OpenSim an inverse dynamics analysis was performed to determine the intersegmental moments before proceeding to muscle force estimation. Generalized actuators acting on the 6 degrees of freedom of the pelvis with respect to the ground reference system were defined in order to provide the dynamic contributions associated with the missing torso and controlateral leg, so equilibrating this segment during the static optimization simulations without influencing muscle recruitment.

2.3 Load sharing problem

The system is statically indeterminate and different combinations of muscle forces are able to satisfy the joint equilibrium when an external moment is applied. A unique solution to the problem of distributing the external load between the actuators can be found by minimizing an appropriate function J of the muscle forces, as proposed in previous works (Seireg and Arvikar, 1973; Penrod et al., 1974; Pedotti et al., 1978; Crowninshield and Brand, 1981). The objective function can be minimized under the constraints of mechanical equilibrium at the joints and physiological limits for muscle tensions, such that the general optimization problem can be expressed as follows:

$$\text{minimize} \quad J(F_i) = \sum_{i=1}^{n} \left(\frac{F_i}{F_{i,max}} \right)^p \tag{1.1}$$

$$\text{subject to} \sum_{i=1}^{n} \vec{r}_{ij} \times \vec{F}_i = \vec{M}_j \qquad i = 1,\ldots,n\,; \qquad j = 1,\ldots,d \tag{1.2}$$

$$0 \le F_i \le F_{i,max} \qquad i = 1,\ldots,n \tag{1.3}$$

where F_i is the magnitude of i-th muscle force, $F_{i,max}$ is the value of the maximal force the *i*-th muscle can exert (here considered to be the maximal isometric force F_{ISO}, calculated as described in section 2.1), p is the power of the objective function, n is the total number of actuators, $\vec{r}_{ij}$ is the moment arm of the i-th muscle with respect to the j-th joint axis, d is the total number of axes in the model and $\vec{M}_j$ is the moment acting around the j-th joint axis. This technique is known as static optimization and solves the muscle load distribution problem for the intersegmental joint moments calculated through the inverse dynamics analysis in each frame of the kinematics independently, as in a statics problem.

By increasing the power of p the muscle synergism is enhanced in the sense that the load is shared more equally in terms of muscle activation between the recruited actuators (Rasmussen et al., 2001). To evaluate the influence of muscle synergism on HCF and muscle force estimation, all powers between $p = 1$ and $p = 15$ were considered.

2.4 Hip contact forces and muscle forces

The numerical HCFs obtained for each adopted power were compared against the HIP98 measurements in terms of relative variability (maximum difference between the cycle force peak and the mean force peak divided by the mean force peak value) and relative deviation (difference between numerical and experimental HCFs divided by the experimental value). The latter parameter was calculated at the instant of the experimental peak (to compare the results with Heller et al. (2001) and Stansfield et al. (2003)) and between the numerical and experimental maximum peaks. When averaging relative deviations, absolute values were considered in order to avoid cancellation due to opposite signs. The time shift between the numerical and experimental peaks (calculated for the first peak and expressed in percentage of the activity cycle) was also determined to assess the reliability of the peak time prediction.

In addition, the root mean square error (RMSE) and the Pearson's product-moment correlation coefficient (R) were calculated for each simulated trial in order to globally assess the model predictions and the similarity in shape of the HCFs profiles, as for a similar validation focused on the upper limb (Nikooyan et al., 2010); ranges are provided for both parameters.

The estimated muscle forces were evaluated against activation profiles available in the literature for level walking (Wootten et al., 1990; Perry, 1992) and stair climbing (McFadyen and Winter, 1988).

3. Results

A visual comparison between the calculated and the experimental resultant HCFs for different values of p is provided in Fig. 2 and Fig. 3 for level walking and stair climbing respectively. When $p = 1$ and $p = 2$ the model both overestimates and underestimates the HCFs compared to *in vivo* measurements, but the tendency is to progressively overestimate the joint contact forces as p increases. This trend is clearly displayed in Fig. 4 where the average HCFs peak values calculated for all the subjects are shown.

The numerical results of the simulations are available from Table 2 and Table 3. The relative variability is on average below 12% for all recruitment criteria for both activities; the relative deviation at experimental peak is on average minimum when $p = 1$ for walking (9.9%) and $p = 2$ for stair climbing (7.8%), while the peak to peak mean deviation is monotonically increasing with the objective function power starting from 18.8% for walking and 8.1% for stair climbing. The RMSE values were at their lowest for $p = 1$ for walking and $p = 2$ for stair climbing, but stronger correlation coefficients were found for $p = 2$ (walking: $0.90 \leq R \leq 0.96$, stair climbing: $0.84 \leq R \leq 0.97$; $p < 0.001$ for all trials). Finally, the timing of the numerical peaks remains relatively consistent, independent of the criterion chosen to solve the load sharing problem (maximum average shift: 8.2% of gait cycle for walking and 5.5% for stair climbing).

Forces in muscles crossing the hip are shown for an example cycle of level walking (Fig. 5) and stair climbing (Fig. 6) for Subject S1. The model recruits a minimum number of muscle bundles with an extremely sparse activation profile for both activities when a linear recruitment is adopted. Higher powers of the objective function enhance muscle synergism, continuity of the activation profiles and complex muscle recruitment features such as co-contraction of antagonistic muscle bundles. The muscle forces produced by nonlinear recruitment criteria present activation profiles more consistent with the experimental EMG data than those resulting from a linear criterion.

4. Discussion

4.1 Hip contact forces

The average relative variability of the experimental HCFs resultant derived from HIP98 data does not exceed 8% for both level walking and stair climbing and is generally reproduced by the HCFs from the model (around 11% when $p < 5$, then decreasing for higher powers). The magnitude of the HCFs clearly depends on the value of p, i.e. on the muscle synergism that the chosen recruitment criterion is able to express. When considering linear optimization (minimal degree of muscle synergism/antagonism), the average relative deviations at the instant of the measured HCFs peak (9.9% for level walking and 11.0% for stair climbing) denotes a better agreement with the measured forces in terms of magnitude than found by Heller et al. (2001) (12% for walking and 14% for stair climbing). Stansfield et al. (2003) predicted similar values (S1: 12.3% and S2: 6.2% for walking) to those obtained in this study but the joint forces calculated here produce a clear double peak profile in comparison to the abnormal third peaked force calculated in their study. It is worth recalling that in this study the absolute value of cycle relative deviations is averaged to avoid cancellations due to opposite signs; if the arithmetic mean was calculated as in Heller et al. (2001) then our average relative deviation would be 3.9% for walking and 10.9% for stair climbing, lower than reported in their study.

By using nonlinear muscle recruitment criteria, the HCFs increase with the power of J as previously reported by Pedersen et al. (1987) comparing linear and cubic objective functions. When the function with the highest power is used (p = 15) the model overestimates the joint contact force peak on average by 183.6% for walking and 159.4% for stair climbing (Table 2 and Table 3). The magnitude increment of the HCFs when raising the power of the objective function can be explained by the interconnected effects of muscle discretization and muscle synergism. As demonstrated in previous investigations (Dul et al., 1984; Rasmussen et al., 2001), the synergism between muscles increases with the objective function power, but the activation of a larger number of actuators also generates moments out of the plane in which the external moments are acting, so forcing other muscles to contract to stabilize the spherical hip joint in response to these additional moments.

4.2 Muscle forces and EMG

The assessment of the predicted muscle forces is based on experimental EMG profiles from healthy subjects available in the literature for level walking (Wootten et al., 1990) and stair climbing (McFadyen and Winter, 1988). However, the staircase inclination was less in the HIP98 trials than in the EMG dataset. Müller et al. (1998) measured EMG activity at the end of single leg stance increasing with the inclination of the staircase for the *glutei* and *rectus femoris*, while medial hamstrings activation (*semitendinosus*) was scarcely influenced. Being aware of the results of that study and considering the modest effect of stair inclination on joint angle and moment patterns (Riener et al., 2002), it was still considered meaningful to compare in a qualitative way the estimated muscle forces with the EMG signals reported by McFadyen and Winter (1988).

As Fig. 5 and Fig. 6 display in column $p = 1$, the linear recruitment criterion does not produce results consistent with the EMG data. As previously observed in the literature (Hardt, 1978), only a few muscle bundles were suddenly recruited and often reached maximum activation e.g. the single bundles of *adductor longus* active around toe off. G*luteus maximus* was not recruited during stair climbing simulation, although its action as a hip extensor is recorded by the EMG data.

When using low power ($p \leq 5$) nonlinear optimization criteria, the monoarticular muscles crossing the hip joint (*gluteus maximus, gluteus medius, adductor longus*) present activation profiles comparable to the EMG patterns for both the investigated activities.

Concerning the hip biarticular muscles, the *semitendinosus* exhibits a profile compatible with the gait EMG pattern (Fig. 5) especially for low power nonlinear criteria, while for stair climbing (Fig. 6) its activation resembles the three-peaked experimental EMG only for $p = 2$, as for higher powers a major fourth peak arises towards the end of single leg stance. The *biceps femoris* (long head) activity peaks during the weight acceptance phase of gait (Fig. 5, fifth row) as the reported EMG profile but then is almost silent till the next heel strike, where only a minor activation increase matches with the second experimental peak at terminal swing. Finally, *rectus femoris* presents a single peak in the pre-swing phase of the gait cycle (Fig. 5, last row), in contrast with the data published by Wootten et al. (1990) but in accordance with those of Perry (1992). During stair climbing simulations, this muscle does not produce force except for an isolated peak just before toe off unless a high power criterion is used (Fig. 6, $p = 10$). In this case, the numerical activation becomes comparable to the EMG data of McFadyen and Winter (1988) and Müller et al. (1998).

In conclusion, when nonlinear recruitment criteria are adopted the model recruits hip muscles with activation patterns that are consistent with EMG measurements for single-joint and most biarticular muscles for both walking and stair climbing. The agreement between EMG and muscle forces has been recognized as a qualitative means of validation for muscle force predictions (Patriarco et al., 1981; Pedersen et al., 1987). If this accordance occurs for hip joint crossing muscles together with reliable prediction of the measured HCFs, it strongly supports the hypothesis that the contact forces were obtained from a set of forces reproducing the actual muscle recruitment. This is the case for the developed model when a quadratic criterion is adopted.

The comparison of the force and EMG profiles for muscles not directly crossing the hip joint is available in the supplementary website material.

4.3 Limitations of the model

In the present model neither contraction dynamics nor force-length-velocity relationships were implemented for the muscle actuators. This has been shown not to influence muscle force prediction for walking (Anderson and Pandy, 2001), but it may be relevant for stair climbing.

Furthermore, although estimated by using kinematics and kinetics from total hip replacement patients, the predicted muscle forces were compared against EMG signals recorded in healthy subjects. This kind of validation can be found in previous works, e.g. Stansfield et al. (2003), and is partially justified since at the time of HIP98 data collection the four patients were on average 17 months post-operative (Bergmann et al., 2001). At this post-operative time, patient gait and EMG patterns have been observed to shift towards normality, although hip muscle weakness (not modeled in our simulations) persists for longer periods (Murray et al., 1981; Long et al., 1993).

Although beyond the immediate scope of this work, the presented model needs to be further assessed in order to quantify the sensitivity of the produced results to possible deviation in the description of the kinematics and in the muscle attachment positions resulting from subject-specific scaling, as well as possible alteration due to surgical treatments (such as total hip replacement of the investigated patients).

5. Summary

A lower limb model has been implemented using the open source software OpenSim and validated for the hip joint using public domain data. The model is capable of predicting reliable hip joint contact forces based on realistic muscle activation patterns using a quadratic objective function. This, together with the high discretization of the broad attachment muscles, makes the model especially valuable in producing biofidelic balanced sets of muscle and joint contact forces, with application in finite element models of the musculoskeletal hip construct (Speirs et al., 2007; Wagner et al., 2010); as well as being of potential use in informing the development of physiotherapy and rehabilitation programs, as the effect on the hip joint of load bearing activities can be assessed.

The developed model is available at the website https://simtk.org/home/low_limb_london.

Conflict of interest statement

None of the authors have any financial or personal conflict of interest with regard to this study.

Acknowledgments

This work was supported by the Engineering and Physical Sciences Research Council (Grant EP/F062761/1).

References

Anderson, F. C. and Pandy, M. G., 2001. Static and dynamic optimization solutions for gait are practically equivalent. Journal of Biomechanics 34, 153-161.

Arnold, E., Ward, S., Lieber, R. and Delp, S., 2010. A Model of the Lower Limb for Analysis of Human Movement. Annals of biomedical engineering 38, 269-279.

Bean, J. C. and Chaffin, D. B., 1988. Biomechanical model calculation of muscle contraction forces: a double linear programming method. Journal of Biomechanics 21, 59-66.

Bergmann, G., Deuretzbacher, G., Heller, M., Graichen, F., Rohlmann, A., Strauss, J. and Duda, G. N., 2001. Hip contact forces and gait patterns from routine activities. Journal of Biomechanics 34, 859-871.

Brand, R. A., Crowninshield, R. D., Wittstock, C. E., Pedersen, D. R., Clark, C. R. and van Krieken, F. M., 1982. A model of lower extremity muscular anatomy. Journal of Biomechanical Engineering 104, 304-310.

Brand, R. A., Pedersen, D. R., Davy, D. T., Kotzar, G. M., Heiple, K. G. and Goldberg, V. M., 1994. Comparison of hip force calculations and measurements in the same patient. Journal of Arthroplasty 9, 45-51.

Brand, R. A., Pedersen, D. R. and Friederich, J. A., 1986. The sensitivity of muscle force predictions to changes in physiologic cross-sectional area. Journal of Biomechanics 19, 589-596.

Cleather, D. J. and Bull, A. M. J., 2010. Lower-extremity musculoskeletal geometry affects the calculation of patellofemoral forces in vertical jumping and weightlifting. Proceedings of the Institution of Mechanical Engineers, Part H: Journal of Engineering in Medicine 224, 1073-1083.

Crowninshield, R. D., 1978. Use of optimization techniques to predict muscle forces. Journal of Biomechanical Engineering 100, 88-92.

Crowninshield, R. D. and Brand, R. A., 1981. A physiologically based criterion of muscle force prediction in locomotion. Journal of Biomechanics 14, 793-801.

Crowninshield, R. D., Johnston, R. C., Andrews, J. G. and Brand, R. A., 1978. A biomechanical investigation of the human hip. Journal of Biomechanics 11, 75-77, 79-85.

Davy, D. T., Kotzar, G. M., Brown, R. H., Heiple, K. G., Goldberg, V. M., Heiple, K. G., Jr., Berilla, J. and Burstein, A. H., 1988. Telemetric force measurements across the hip after total arthroplasty. The Journal of Bone and Joint Surgery (American Edition) 70, 45-50.

Delp, S. L., Loan, J. P., Hoy, M. G., Zajac, F. E., Topp, E. L. and Rosen, J. M., 1990. An interactive graphics-based model of the lower extremity to study orthopaedic surgical procedures. IEEE Transactions on Biomedical Engineering 37, 757-767.

Dul, J., Townsend, M. A., Shiavi, R. and Johnson, G. E., 1984. Muscular synergism--I. On criteria for load sharing between synergistic muscles. Journal of Biomechanics 17, 663-673.

Glitsch, U. and Baumann, W., 1997. The three-dimensional determination of internal loads in the lower extremity. Journal of Biomechanics 30, 1123-1131.

Hardt, D. E., 1978. Determining muscle forces in the leg during normal human walking - An application and evaluation of optimization methods. Journal of Biomechanical Engineering 100, 72-78.

Haxton, H. A., 1944. Absolute muscle force in the ankle flexors of man. Journal of Physiology 103, 267-273.

Heller, M. O., Bergmann, G., Deuretzbacher, G., Dürselen, L., Pohl, M., Claes, L., Haas, N. P. and Duda, G. N., 2001. Musculo-skeletal loading conditions at the hip during walking and stair climbing. Journal of Biomechanics 34, 883-893.

Klein Horsman, M. D., 2007. The Twente Lower Extremity Model. PhD Thesis, University of Twente, Twente.

Klein Horsman, M. D., Koopman, H. F., van der Helm, F. C., Prose, L. P. and Veeger, H. E., 2007. Morphological muscle and joint parameters for musculoskeletal modelling of the lower extremity. Clinical Biomechanics 22, 239-247.

Koopman, H. F. J. M. and Klein Horsman, M. D., 2008. Hip compression force estimation with a comprehensive musculoskeletal model. In: Spink, A. J., Ballintijn, M. R., Bogers, N. D., Grieco, F., Loijens, L. W. S., Noldus, L. P. J. J., Smit, G. and Zimmermann, P. H. (Eds), Proceeding of Measuring Behavior 2008, 6th Conference on Methods and Techniques in Behavioural Research. Maastricht, The Netherlands, pp. 16.

Lenaerts, G., De Groote, F., Demeulenaere, B., Mulier, M., Van der Perre, G., Spaepen, A. and Jonkers, I., 2008. Subject-specific hip geometry affects predicted hip joint contact forces during gait. Journal of Biomechanics 41, 1243-1252.

Long, W. T., Dorr, L. D., Healy, B. and Perry, J., 1993. Functional Recovery of Noncemented Total Hip Arthroplasty. Clinical Orthopaedics and Related Research 288, 73-77.

Lu, T. W. and O'Connor, J. J., 1999. Bone position estimation from skin marker co-ordinates using global optimisation with joint constraints. Journal of Biomechanics 32, 129-134.

Lu, T. W., O'Connor, J. J., Taylor, S. J. G. and Walker, P. S., 1997. Validation of a lower limb model with in vivo femoral forces telemetered from two subjects. Journal of Biomechanics 31, 63-69.

McFadyen, B. J. and Winter, D. A., 1988. An integrated biomechanical analysis of normal stair ascent and descent. Journal of Biomechanics 21, 733-744.

Morlock, M., Schneider, E., Bluhm, A., Vollmer, M., Bergmann, G., Müller, V. and Honl, M., 2001. Duration and frequency of every day activities in total hip patients. Journal of Biomechanics 34, 873-881.

Müller, R., Bisig, A., Kramers, I. and Stüssi, E., 1998. Influence of stair inclination on muscle activity in normals. Journal of Biomechanics 31, Supplement 1, 32.

Murray, M. P., Gore, D. R., Brewer, B. J., Mollinger, L. A. and Sepic, S. B., 1981. Joint Function after Total Hip Arthroplasty: A Four-Year Follow-Up of 72 Cases with Charnley and Müller Replacements. Clinical Orthopaedics and Related Research 157, 119-124.

Nikooyan, A. A., Veeger, H. E. J., Westerhoff, P., Graichen, F., Bergmann, G. and van der Helm, F. C. T., 2010. Validation of the Delft Shoulder and Elbow Model using in-vivo glenohumeral joint contact forces. Journal of Biomechanics 43, 3007-3014.

Patriarco, A. G., Mann, R. W., Simon, S. R. and Mansour, J. M., 1981. An evaluation of the approaches of optimization models in the prediction of muscle forces during human gait. Journal of Biomechanics 14, 513-525.

Paul, J. P., 1965. Bioengineering studies of the forces transmitted by joints-II. In: Kenedi, R. M. (Ed), Biomechanics and Related Bioengineering Topics. Pergamon press, Oxford, pp. 369-380.

Pedersen, D. R., Brand, R. A., Cheng, C. and Arora, J. S., 1987. Direct comparison of muscle force predictions using linear and nonlinear programming. Journal of Biomechanical Engineering 109, 192-200.

Pedotti, A., Krishnan, V. V. and Stark, L., 1978. Optimization of muscle-force sequencing in human locomotion. Mathematical Biosciences 38, 57-76.

Penrod, D. D., Davy, D. T. and Singh, D. P., 1974. An optimization approach to tendon force analysis. Journal of Biomechanics 7, 123-129.

Perry, J., 1992. Hip. In: Gait Analyis: Normal and Pathologic Function. SLACK Incorporated, Thorofare, NJ USA, pp. 111-129.

Rasmussen, J., Damsgaard, M. and Voigt, M., 2001. Muscle recruitment by the min/max criterion -- a comparative numerical study. Journal of Biomechanics 34, 409-415.

Riener, R., Rabuffetti, M. and Frigo, C., 2002. Stair ascent and descent at different inclinations. Gait & Posture 15, 32-44.

Röhrle, H., Scholten, R., Sigolotto, C., Sollbach, W. and Kellner, H., 1984. Joint forces in the human pelvis-leg skeleton during walking. Journal of Biomechanics 17, 409-424.

Rydell, N. W., 1966. Forces acting on the femoral head-prosthesis. A study on strain gauge supplied prostheses in living persons. Acta orthopaedica Scandinavica 37, Supplement 88, 81-132.

Seireg, A. and Arvikar, R. J., 1973. A mathematical model for evaluation of forces in lower extremeties of the musculo-skeletal system. Journal of Biomechanics 6, 313-326.

Seireg, A. and Arvikar, R. J., 1975. The prediction of muscular load sharing and joint forces in the lower extremities during walking. Journal of Biomechanics 8, 89-102.

Speirs, A. D., Heller, M. O., Duda, G. N. and Taylor, W. R., 2007. Physiologically based boundary conditions in finite element modelling. Journal of Biomechanics 40, 2318-2323.

Stansfield, B. W., Nicol, A. C., Paul, J. P., Kelly, I. G., Graichen, F. and Bergmann, G., 2003. Direct comparison of calculated hip joint contact forces with those measured using instrumented implants. An evaluation of a three-dimensional mathematical model of the lower limb. Journal of Biomechanics 36, 929-936.

Van der Helm, F. C. and Veenbaas, R., 1991. Modelling the mechanical effect of muscles with large attachment sites: application to the shoulder mechanism. Journal of Biomechanics 24, 1151-1163.

Wagner, D. W., Divringi, K., Ozcan, C., Grujicic, M., Pandurangan, B. and Grujicic, A., 2010. Combined musculoskeletal dynamics/structural finite element analysis of femur physiological loads during walking. Multidiscipline Modeling in Materials and Structures 6, 417-437.

Weijs, W. A. and Hillen, B., 1985. Cross-sectional areas and estimated intrinsic strength of the human jaw muscles. Acta morphologica neerlando-scandinavica 23, 267-274.

Wootten, M., Kadaba, M. and Cochran, G., 1990. Dynamic electromyography. II. Normal patterns during gait. Journal of Orthopaedic Research 8, 259-265.

Wu, G., Siegler, S., Allard, P., Kirtley, C., Leardini, A., Rosenbaum, D., Whittle, M., D'Lima, D. D., Cristofolini, L., Witte, H., Schmid, O. and Stokes, I., 2002. ISB recommendation on definitions of joint coordinate system of various joints for the reporting of human joint motion - part I: ankle, hip, and spine. Journal of Biomechanics 35, 543-548.

Yeo, B. P., 1976. Investigations concerning the principle of minimal total muscular force. Journal of Biomechanics 9, 413-416.

Figure 1 The musculoskeletal model as implemented in OpenSim.

Figure 2 Comparison between the average resultant of measured HCFs (in red) and numerical HCFs (in black) for level walking. Numerical HCFs are calculated for each subject available in the HIP98 using several values of the power of the objective function *p* and considering all the activity trials. The thin lines represent one standard deviation with respect to the average value.

Figure 3 Comparison between the average resultant of measured HCFs (in red) and numerical HCFs (in black) for stair climbing. Numerical HCFs are calculated for each subject available in the HIP98 using several values of the power of the objective function *p* and considering all the activity trials. The thin lines represent one standard deviation with respect to the average value.

Figure 4 Sensitivity of the mean value of the maximum HCFs calculated from all the trials for each subject to the power of the objective function, *p*.

Figure 5 Comparison between the EMG profiles for walking published by Wootten et al. (1990) (grey shaded areas, activity scale between 0 and 1 on the left side of the plots) and the muscle forces of an example gait trial of Subject S1 (thin black lines, force scale on the right side of the plots) estimated using different objective functions. Only hip crossing muscles are represented: *gluteus maximus* (8 selected bundles), *gluteus medius* (12 bundles), *adductor longus* (6 bundles), *semitendinosus* (single bundle), *biceps femoris caput* *longum* (single bundle), *rectus femoris* (2 bundles). Toe off is indicated with a thin red line in each subplot.

Figure 6 Comparison between the EMG profiles for stair climbing published by McFadyen and Winter (1988) (grey shaded areas, activity scale between 0 and 1 on the left side of the plots) and the muscle forces of an example gait trial of Subject S1 (thin black lines, force scale on the right side of the plots) estimated using different objective functions. Only hip crossing muscles are represented: *gluteus maximus inferior* (6 bundles), *gluteus medius* (12 bundles), *semitendinosus* (single bundle), *rectus femoris* (2 bundles). Toe off is indicated with a thin red line in each subplot.

Table 1

General characteristic of patients and the recorded experimental trials available on the HIP98 database.

Table 2

Results of the level walking simulations in terms of relative variability, relative deviation (calculated at the frame of experimental peak and between the numerical and experimental peak), peak time shift, range of the root mean square error (RMSE) and Pearson's correlation coefficient ($p < 0.001$ for all trials). The absolute value of the relative deviations was used when averaging the result of different trials.

[†] indicates underestimation of the experimental peak determined with the arithmetical mean of the relative deviations.

[*]indicates delay of the numerical peak with respect to the experimental.

Table 3

Results of the stair climbing simulations in terms of relative variability, relative deviation (calculated at the frame of experimental peak and between the numerical and experimental peak), peak time shift, range of the root mean square error (RMSE) and Pearson's correlation coefficient ($p < 0.001$ for all trials). The absolute value of the relative deviations was used when averaging the result of different trials.

[†] indicates underestimation of the experimental peak determined with the arithmetical mean of the relative deviations.

[*]indicates delay of the numerical peak with respect to the experimental.

Figure 1

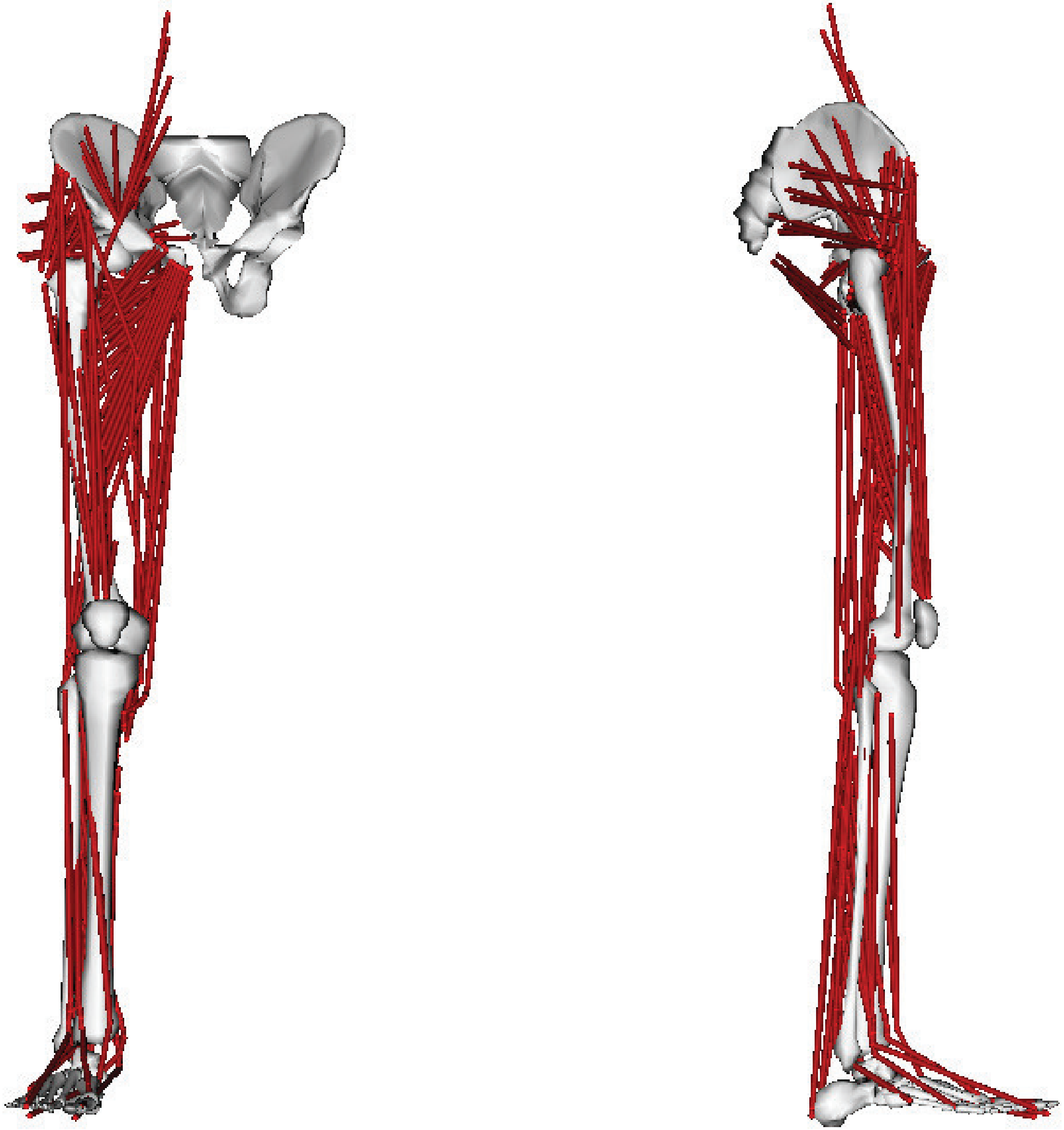

Figure 2

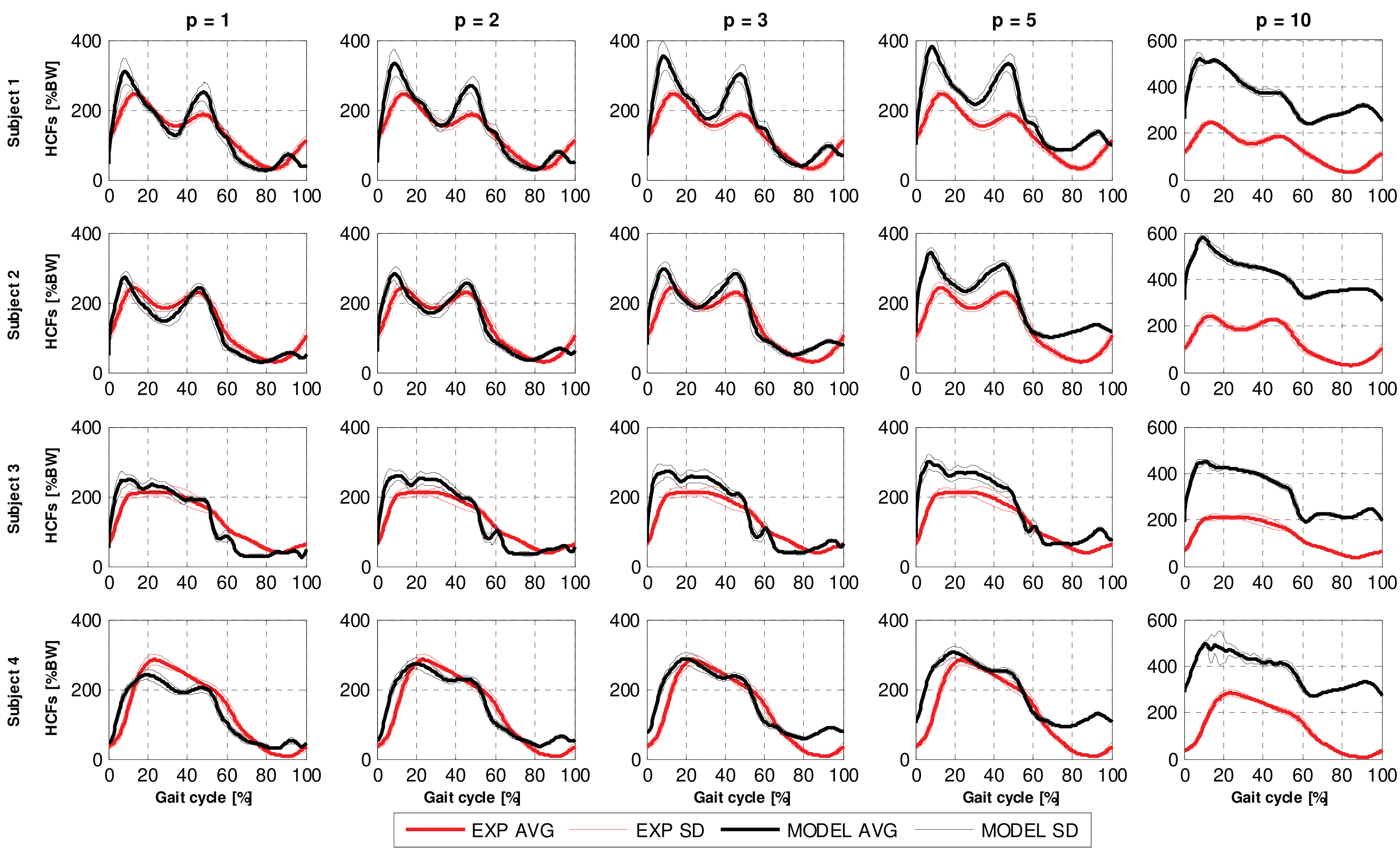
p = 1
p = 2
p = 3
p = 5
p = 10
Subject 1
Subject 2
Subject 3
Subject 4
HCFs [%BW]
Gait cycle [%]
EXP AVG
EXP SD
MODEL AVG
MODEL SD

Figure 3

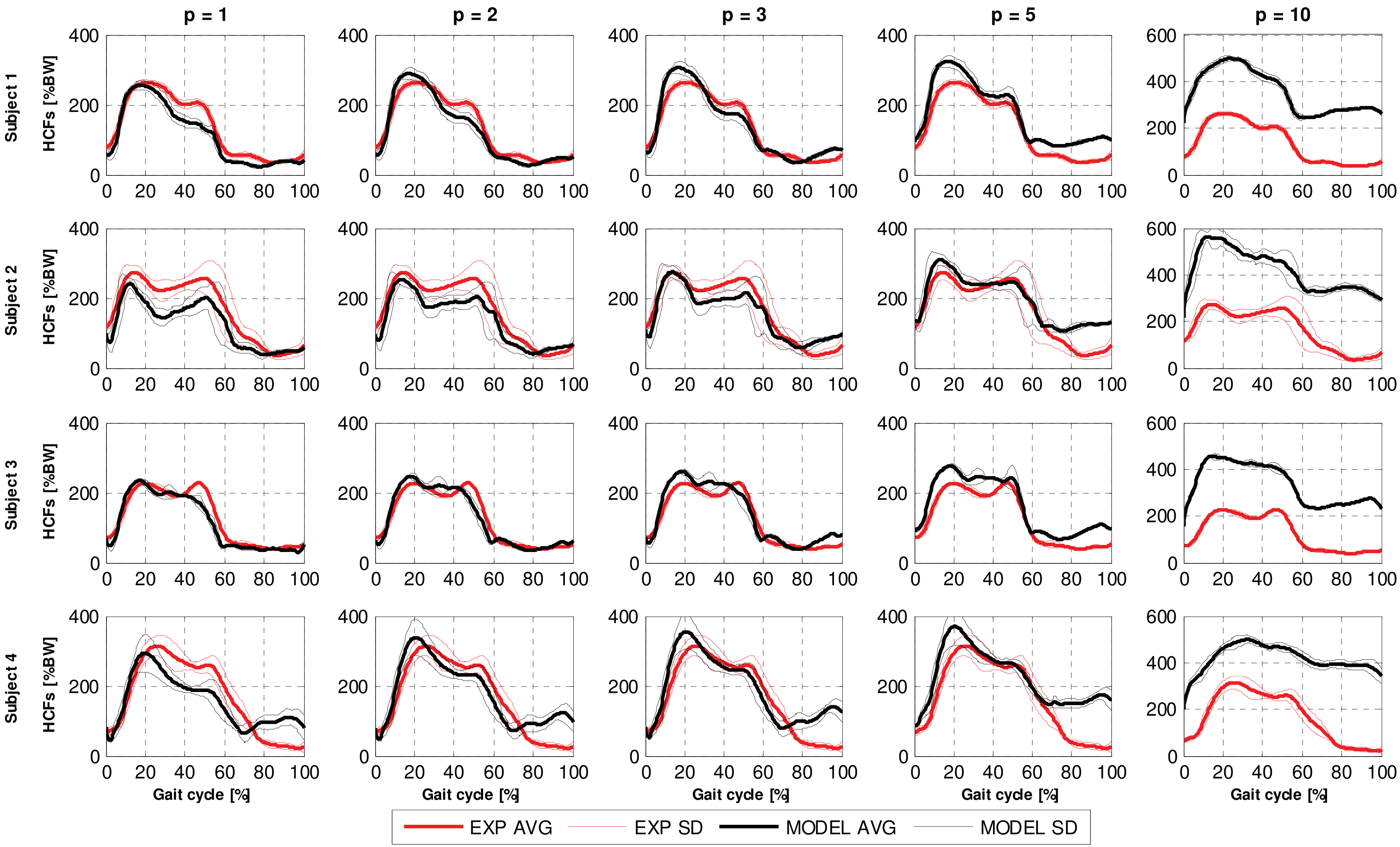
p = 1
p = 2
p = 3
p = 5
p = 10
Subject 1
Subject 2
Subject 3
Subject 4
HCFs [%BW]
Gait cycle [%]
EXP AVG
EXP SD
MODEL AVG
MODEL SD

Figure 4

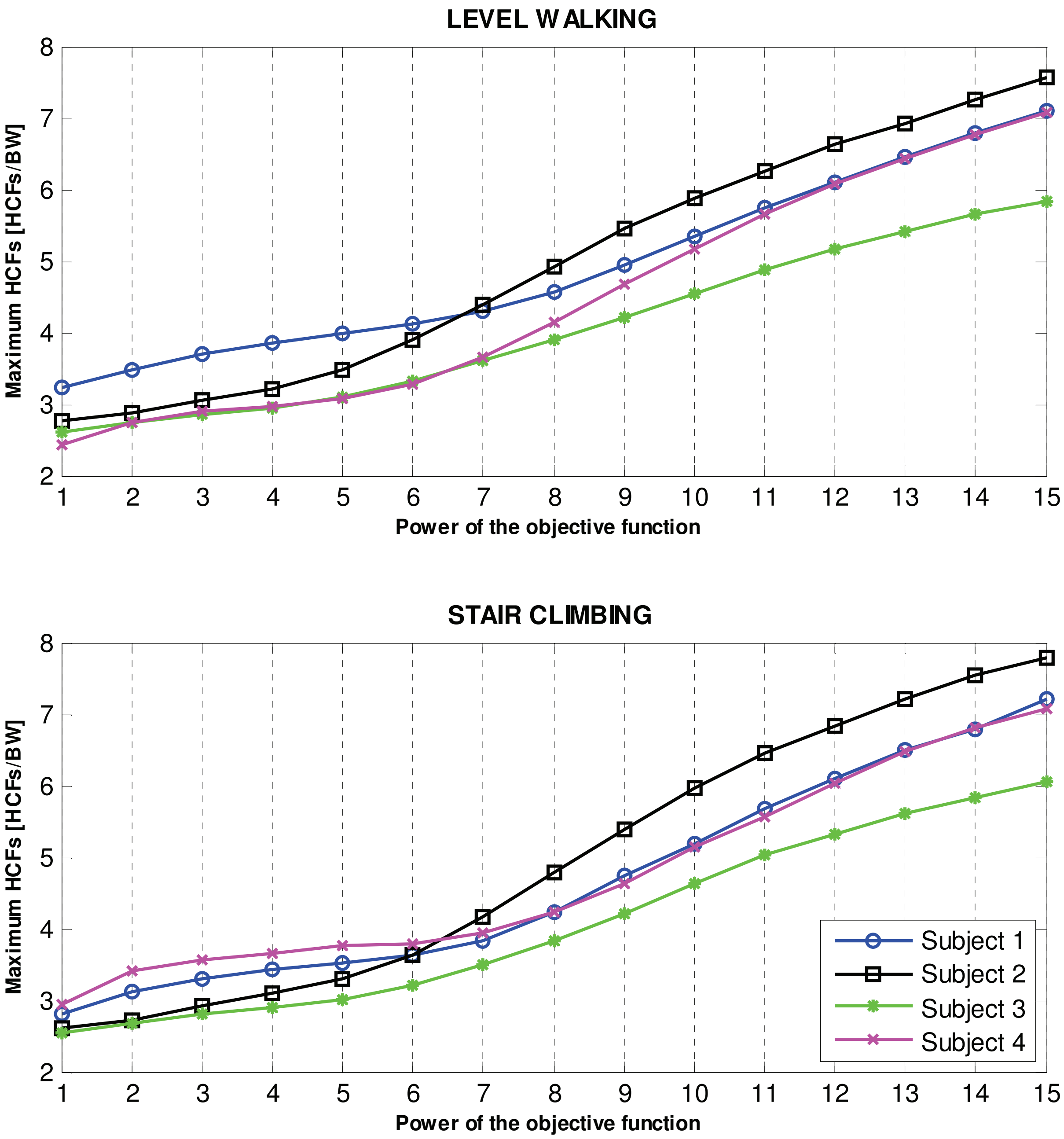

LEVEL WALKING
Maximum HCFs [HCFs/BW]
Power of the objective function
STAIR CLIMBING
Maximum HCFs [HCFs/BW]
Power of the objective function
Subject 1
Subject 2
Subject 3
Subject 4

Figure 5

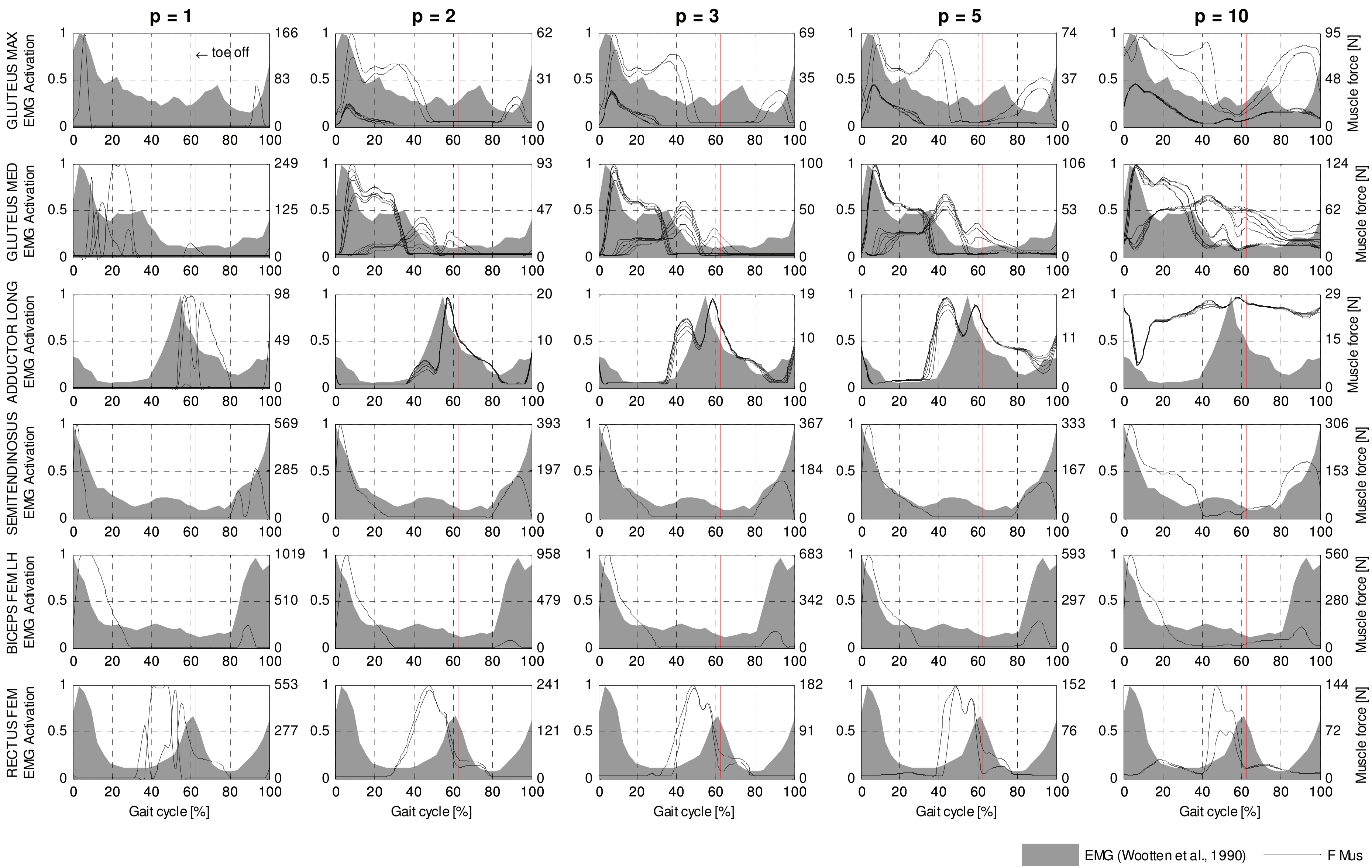
p = 1
p = 2
p = 3
p = 5
p = 10
GLUTEUS MAX
GLUTEUS MED
ADDUCTOR LONG
SEMITENDINOSUS
BICEPS FEM LH
RECTUS FEM
EMG Activation
Muscle force [N]
← toe off
Gait cycle [%]
EMG (Wootten et al., 1990)
F Mus

Figure 6

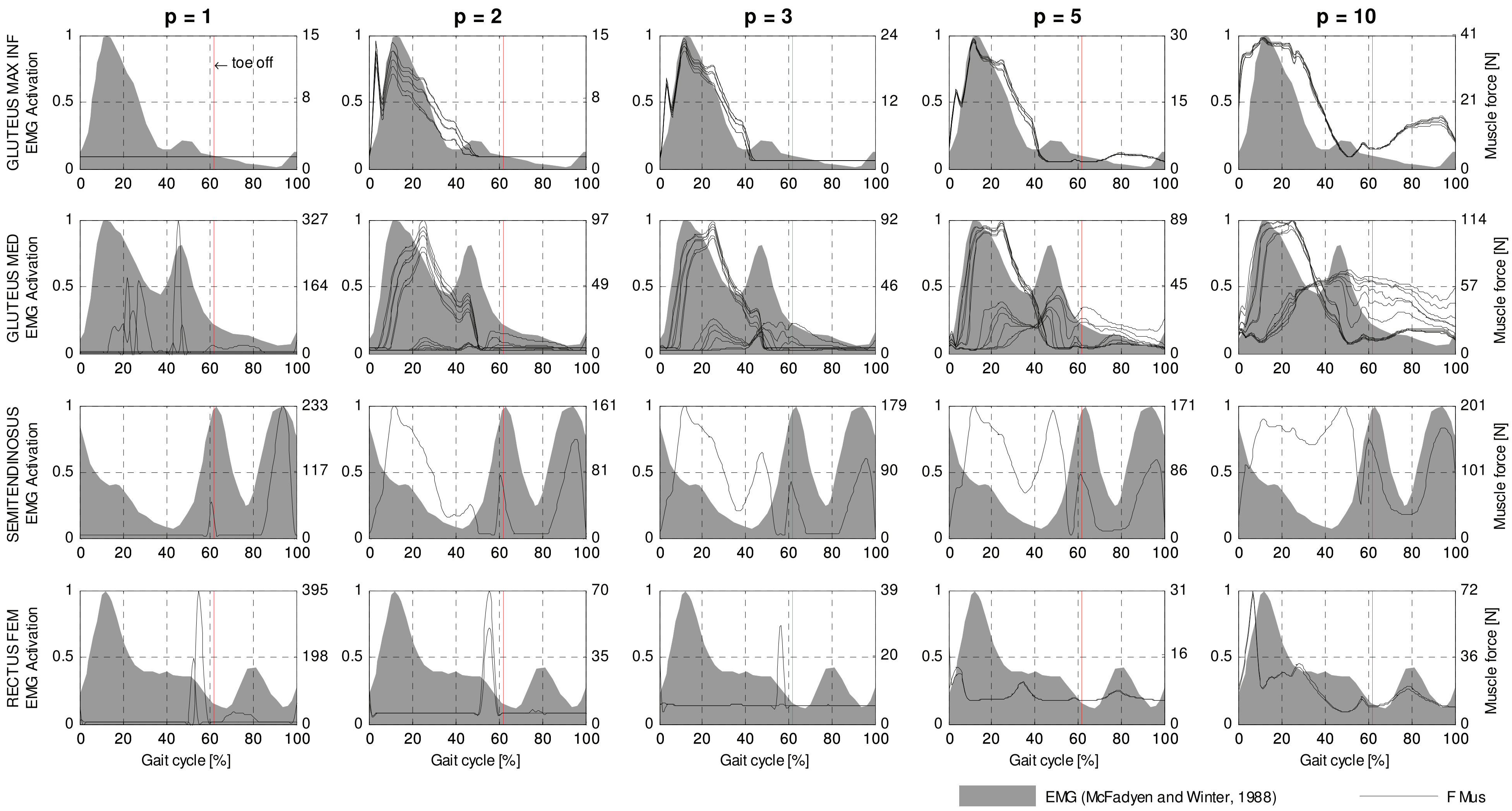

p = 1
p = 2
p = 3
p = 5
p = 10
GLUTEUS MAX INF EMG Activation
GLUTEUS MED EMG Activation
SEMITENDINOSUS EMG Activation
RECTUS FEM EMG Activation
Muscle force [N]
← toe off
Gait cycle [%]
EMG (McFadyen and Winter, 1988)
F Mus

Table

Table 1

Subject	HIP98 name	Sex	Age	Body Weight [N]	Height [m]	Walking speed [m/s]	Walking trials	Stair Climbing mean time [s]	Stair Climbing trials
S1	HSR	M	55	860	1.74	1.36	8	1.6	6
S2	KWR	M	61	702	1.65	1.15	8	1.7	6
S3	PFL	M	51	980	1.75	1.13	6	1.5	2
S4	IBL	F	76	800	1.70	1.08	5	1.8	6

Table 2

Subjects	HCFs		P=1	P=2	P=3	P=5	P=10	P=15
S1	**Relative variability**	**[% Exp peak]**	15.9	15.1	16.1	15.8	6.4	3.8
	Rel dev at exp peak	**[% Exp peak]**	6.9	16.7	22.9	30.9	104.7	177.4
	Rel dev betw peaks	**[% Exp peak]**	29.2	39.3	47.7	59.7	114.5	184.6
	Peak time shift	**[% gait cycle]**	5.0	4.5	4.9	5.1	4.5	3.9
	RMSE range	**[%BW]**	29.7-46.7	36.5-52.4	51.0-66.3	73.7-90.6	227.5-235.1	360.1-370.6
	R range		0.90-0.93	0.91-0.94	0.90-0.94	0.88-0.91	0.78-0.85	0.67-0.77
S2	**Relative variability**		7.7	9.0	8.7	5.3	4.6	14.4
	Rel dev at exp peak		9.0†	6.3	9.1	19.5	124.5	187.4
	Rel dev betw peaks		12.4	17.2	24.0	41.5	139.8	241.4
	Peak time shift		5.3	5.3	5.7	6.0	4.1	8.3*
	RMSE range		25.0-35.6	23.2-35.9	32.8-49.1	68.6-78.6	269.0-284.9	426.4-452.3
	R range		0.90-0.96	0.90-0.96	0.87-0.95	0.86-0.93	0.76-0.86	0.57-0.77
S3	**Relative variability**		13.0	12.7	12.7	10.9	4.3	4.8
	Rel dev at exp peak		6.0	11.0	14.2	20.0	85.7	134.6
	Rel dev betw peaks		18.0	22.6	27.6	39.0	103.1	161.2
	Peak time shift		14.9	10.4	10.4	14.5	14.2	13.7
	RMSE range		31.3-39.0	32.9-46.4	38.6-53.5	50.3-65.1	177.3-195.4	287.7-309.7
	R range		0.90-0.94	0.91-0.94	0.89-0.93	0.88-0.93	0.89-0.93	0.81-0.89
S4	**Relative variability**		8.7	8.2	7.6	6.9	1.8	3.2
	Rel dev at exp peak		17.7†	6.3†	4.7†	6.1	71.4	116.6
	Rel dev betw peaks		15.4†	4.1†	3.3	7.2	80.6	147.3
	Peak time shift		3.7	3.4	3.4	3.6	7.1	7.1
	RMSE range		37.1-46.1	33.5-42.9	42.3-52.2	64.8-72.7	235.5-246.6	369.0-400.5
	R range		0.91-0.94	0.91-0.95	0.89-0.94	0.86-0.90	0.67-0.83	0.39-0.63
Average	**Relative variability**		11.3	11.2	11.3	9.7	4.3	6.5
	Rel dev at exp peak		9.9†	10.1	12.7	19.1	96.6	154.0
	Rel dev betw peaks		18.8	20.8	25.7	36.8	109.5	183.6
	Peak time shift		7.2	5.9	6.1	7.3	7.5	8.2
	RMSE total range		25.0-46.7	23.2-52.4	32.8-66.3	50.3-90.6	177.3-284.9	287.7-452.3
	R total range		0.90-0.96	0.90-0.96	0.87-0.95	0.86-0.93	0.67-0.93	0.39-0.89

Table 3

Subjects	HCFs		P=1	P=2	P=3	P=5	P=10	P=15
S1	**Relative variability**	**[% Exp peak]**	7.0	7.9	8.4	7.1	2.1	4.0
	Rel dev at exp peak	**[% Exp peak]**	3.9†	8.4	14.3	21.3	85.3	151.2
	Rel dev betw peaks	**[% Exp peak]**	2.4†	10.6	16.7	23.6	92.9	171.5
	Peak time shift	**[% gait cycle]**	2.2	2.6	2.7	2.7	5.1*	4.1*
	RMSE range	**[%BW]**	29.8-33.3	23.3-29.8	25.7-33.0	41.6-47.6	215.6-228.7	358.3-373.2
	R range		0.96-0.98	0.96-0.97	0.95-0.96	0.96-0.97	0.93-0.96	0.89-0.92
S2	**Relative variability**		13.4	15.2	14.2	9.3	6.3	4.8
	Rel dev at exp peak		19.1†	11.0†	6.9†	10.7	96.1	170.6
	Rel dev betw peaks		13.4†	9.3†	5.1†	10.5	101.6	166.5
	Peak time shift		5.1	4.1	3.8	3.8	3.0	4.0
	RMSE range		44.8-61.2	31.2-47.5	31.6-40.5	38.5-54.4	235.3-274.1	381.0-444.9
	R range		0.94-0.95	0.94-0.97	0.91-0.95	0.90-0.96	0.62-0.93	0.46-0.86
S3	**Relative variability**		0.9	2.1	1.8	1.3	1.9	1.0
	Rel dev at exp peak		3.8†	4.2	11.1	18.6	96.9	171.9
	Rel dev betw peaks		3.3	9.0	14.4	21.9	104.6	178.2
	Peak time shift		3.5	3.2	3.2	2.7	5.7	2.2
	RMSE range		21.7-29.7	20.0-26.8	24.1-28.2	40.8-41.9	207.1-214.3	334.9-340.3
	R range		0.94-0.97	0.94-0.97	0.94-0.98	0.96-0.98	0.95-0.95	0.85-0.87
S4	**Relative variability**		25.2	20.1	18.3	18.2	4.3	3.8
	Rel dev at exp peak		17.4†	7.8†	7.3	8.7	51.5	108.3
	Rel dev betw peaks		13.5†	11.0	11.6	17.5	60.7	121.5
	Peak time shift		6.6	5.2	4.9	4.8	8.4*	6.6*
	RMSE range		59.7-65.5	43.7-61.1	46.9-67.6	65.9-85.2	242.4-279.8	389.3-423.6
	R range		0.76-0.91	0.84-0.92	0.84-0.91	0.83-0.92	0.70-0.83	0.33-0.60
Average	**Relative variability**		11.6	11.3	10.7	9.0	3.6	3.4
	Rel dev at exp peak		11.0†	7.8†	9.9	14.8	82.5	150.5
	Rel dev betw peaks		8.1†	10.0	12.0	18.4	90.0	159.4
	Peak time shift		4.4	3.8	3.6	3.5	5.5*	4.2*
	RMSE total range		21.7-65.5	20.0-61.1	24.1-67.6	38.5-85.2	207.1-279.8	334.9-444.9
	R total range	**[total range]**	0.76-0.98	0.84-0.97	0.84-0.98	0.83-0.98	0.62-0.96	0.33-0.92

Muscle Forces versus EMG patterns for muscles not crossing the hip joint (Figure A and Figure B)

When a linear optimization criterion is adopted, only two bundles of *vastus lateralis* are recruited from the *vasti* muscles both for walking simulation (Fig. A) and stair climbing (Fig. B); the *gastrocnemii* are maximally activated during the propulsive phase of gait although the agonist *soleus* bundles (not represented in Fig. A) are inactive.

When level walking is simulated using nonlinear criteria with p>2, *vastus lateralis* and *vastus medialis* are synchronized in a double peaked action delayed by around 5% of the gait cycle in comparison to the EMG data. The activation profiles of these muscles do not reproduce the EMG peak due to knee extension in preparation of heel strike at the end of the gait cycle. The simplified patellar mechanism implemented in the model could have a role in this inaccurate prediction.

For ankle crossing muscles, any nonlinear recruitment criterion yields activations in remarkable agreement with the experimental EMG measurements for both activities. In particular, the good accordance between muscle force and EMG pattern of the *soleus* displayed in Fig. B, (third row) suggests that the model can reproduce the body lifting and pulling-up action of this muscle during the stance phase of stair climbing.

Co-contraction of the antagonist muscles *tibialis anterior* and *gastrocnemius* is predicted by the present model for higher objective function powers in both the investigated activities.

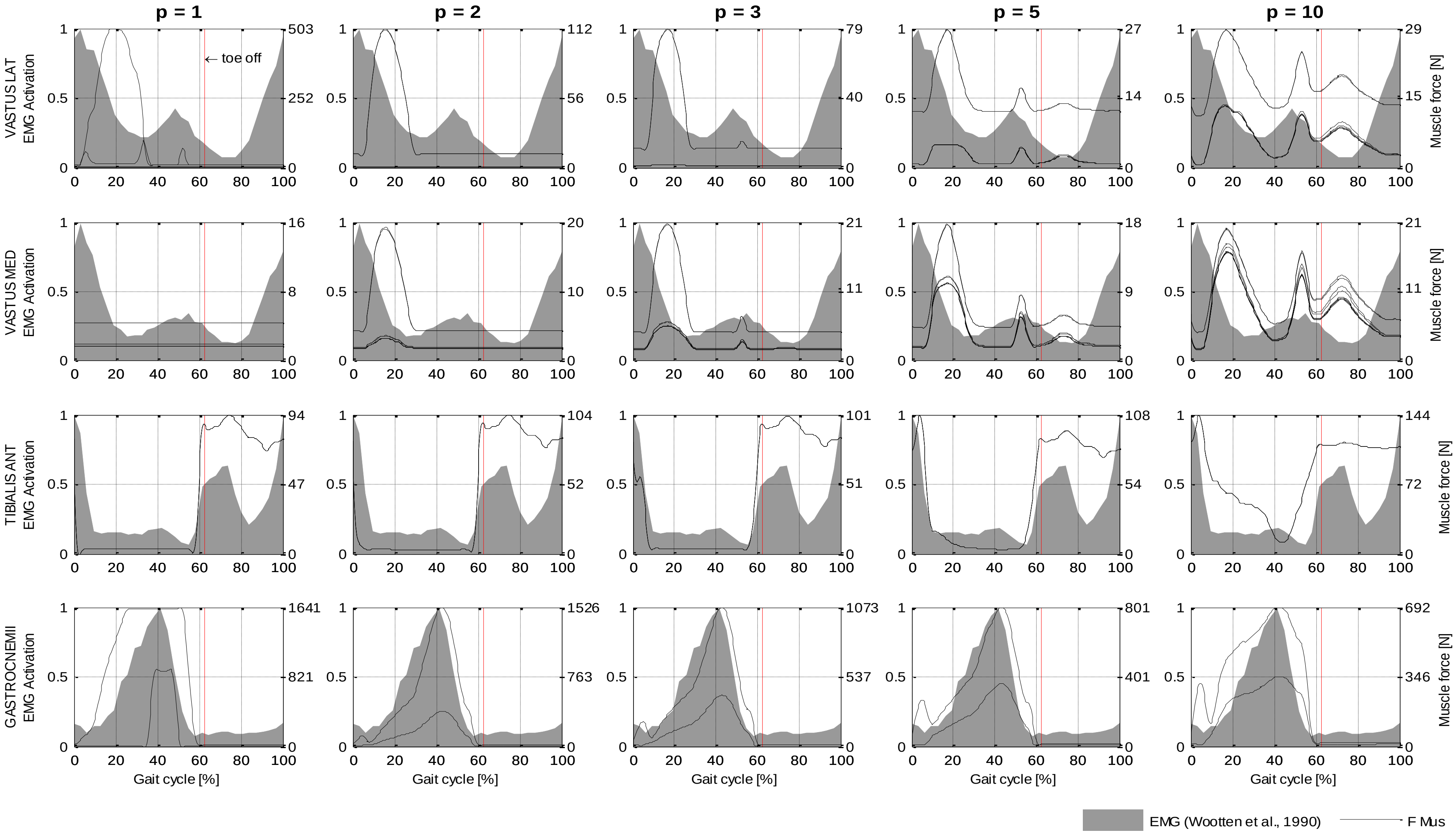

p = 1
p = 2
p = 3
p = 5
p = 10
VASTUS LAT
VASTUS MED
TIBIALIS ANT
GASTROCNEMII
EMG Activation
Muscle force [N]
← toe off
Gait cycle [%]
EMG (Wootten et al., 1990)
F Mus

Figure A

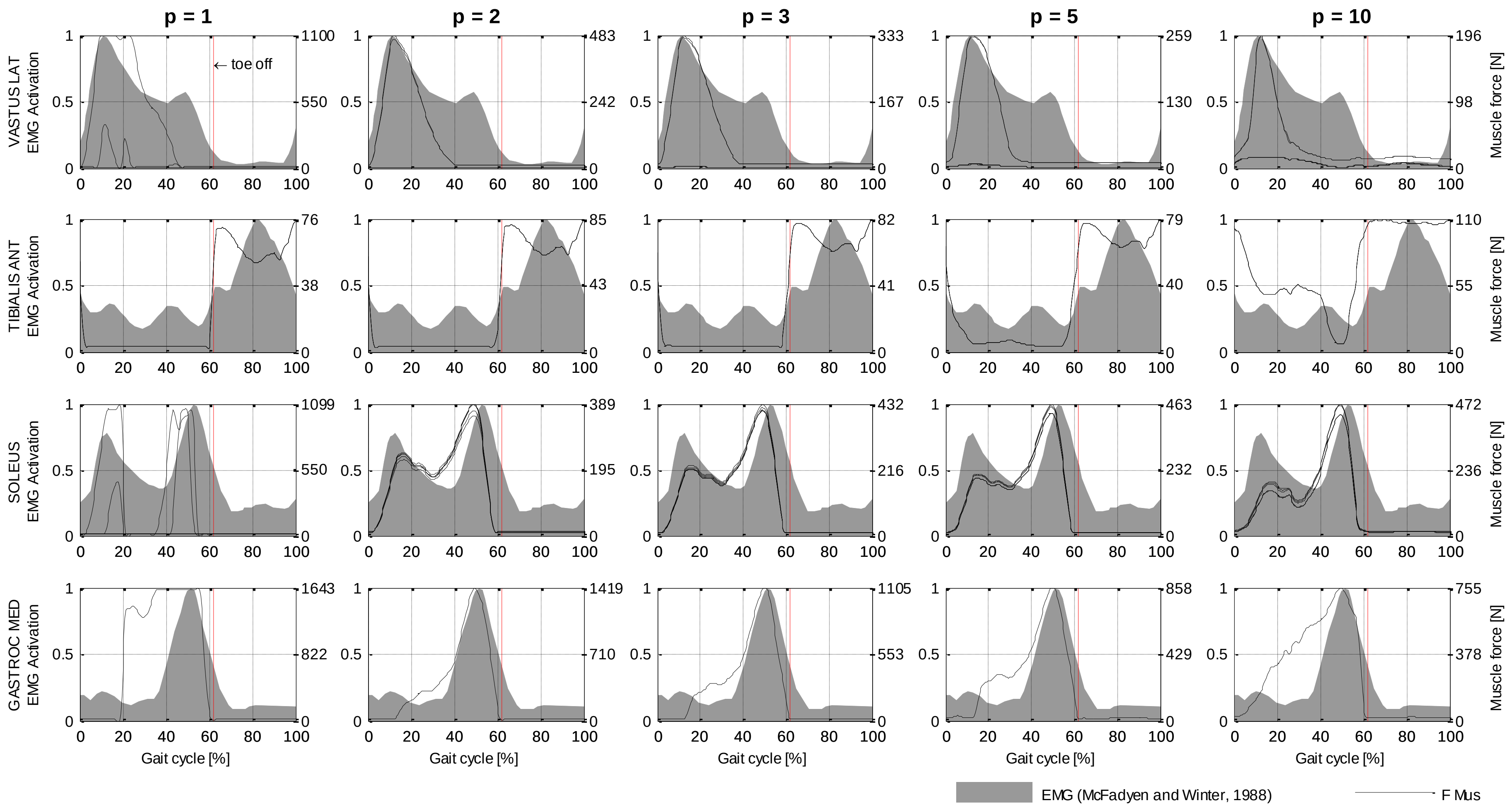
p = 1
p = 2
p = 3
p = 5
p = 10
VASTUS LAT
EMG Activation
TIBIALIS ANT
EMG Activation
SOLEUS
EMG Activation
GASTROC MED
EMG Activation
Muscle force [N]
← toe off
Gait cycle [%]
EMG (McFadyen and Winter, 1988)
F Mus

Figure B